JACS
JOURNAL OF THE AMERICAN CHEMICAL SOCIETY

Article

pubs.acs.org/JACS

Probing the Effect of the Solution Environment around Redox-Active Moieties Using Rigid Anthraquinone Terminated Molecular Rulers

Nadim Darwish,[†] Paul K. Eggers,[†] Simone Ciampi,[†] Yujin Tong,[‡] Shen Ye,*[,‡] Michael N. Paddon-Row,*[,†] and J. Justin Gooding*[,†]

[†]School of Chemistry, The University of New South Wales, Sydney, NSW, 2052, Australia

[‡]Catalysis Research Centre, Hokkaido University, Sapporo 001-0021, Japan

Supporting Information

ABSTRACT: Herein, we report the influence of the position and the solution environment around surface-bound redox-active moieties on their redox reaction. The study was made possible by using rigid norbornylogous bridges, which possess anthraquinone (AQ) moieties. An L-shaped norbornylogous bridge (L-NB) and straight-shaped norbornylogous bridge (S-NB) were used to situate AQ moieties at well-defined position and environments above a mixed alkanethiol self-assembled monolayer (SAM) on Au (111) surfaces. Sum frequency generation (SFG) vibrational spectroscopy was employed to evaluate the interaction between the S-NB and L-NB with diluent molecules in the mixed SAMs. The SFG measurements demonstrated that hydrogen-bonding interactions were formed between AQ moieties of L-NB and diluent molecules terminated by hydroxyl group within a suitable separation. The SFG observations provided information about the relative position of the AQ moieties in each SAM, which significantly affects the thermodynamics and the kinetics of the electron transfer on the electrode/solution interface. The rate constant (k_{et}) of the electron transfer between the AQ moiety and the gold surface and the apparent formal potential ($E^{0\prime}$) were studied using cyclic voltammetry (CV), alternating current voltammetry (ACV), and electrochemical impedance spectroscopy (EIS). It was found that the k_{et} increases and $E^{0\prime}$ shifts to more anodic values as the distance between the AQ moiety and the surface of the diluent was increased, for both methyl and hydroxyl terminated diluent. These results are discussed in relation to H-bonding interactions with water surrounding the AQ moieties.

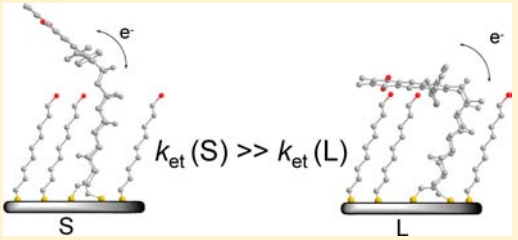

1. INTRODUCTION

Redox-active species attached to electrodes via an organic layer are important in biosensors, fuel cells, photovoltaic devices, protein electrochemistry, and fundamental studies on electron transfer.[1,2] The surface on which the organic layer is attached can have a profound effect on the electron transfer behavior. For instance, using conventional alkanethiol as the base layer of redox-active monolayers, the redox species are located at the organic layer−solution interface, which is essentially within the electrical double layer.[3−5] In an electrochemical experiment, the redox-active species will not feel the potential difference between the working electrode and the reference electrode, but something between as determined by the nature of the electrical double layer. The effect of the electrical double layer on surface-bound redox-active groups was first proposed by the theory of interfacial potential distribution of Smith and White[3] and expanded by Fawcett.[4] In that theory, Smith and White proposed that the potential difference between the plane of the redox-active groups and the bulk solution (i.e., across the double layer) should be included in the Nernst equation.

$$E = E^0 + (\varphi_{PET} - \varphi_{SOL}) + \frac{RT}{nF} \ln\left[\frac{\Gamma_O}{\Gamma_R}\right] \quad (1)$$

The measured potential difference is $E = (\phi_{METAL} - \phi_{REF})$. ϕ_{PET} and ϕ_{SOL} are the potentials of the plane of electron transfer (PET) and the bulk solution, respectively.[3]

The term that is independent of surface coverage in eq 1 is not the formal potential, as in a classical Nernst formula, but $E^0 + (\phi_{PET} - \phi_{SOL})$, which we refer to as the apparent formal potential $E^{0\prime}$. $E^{0\prime}$ is the quantity that is measured in a typical electrochemical experiment. The potential drop across the electrical double layer can be obtained from measurements of the apparent formal potential of modified electrodes, which are constructed with each PET at a different distance from the distal surface of the SAM. As the PET becomes further away from the distal end of the SAM, $\phi_{PET} - \phi_{SOL}$ and hence the apparent formal potential, $E^0 + (\phi_{PET} - \phi_{SOL})$, will decrease by the drop in potential of the electrical double layer between the two points.

We have recently experimentally verified this theory using rigid ferrocene-terminated norbornylogous (NB) bridges that served as molecular rulers for probing the electrical double layer.[5] The importance of rigidity of the NB bridge is that the position of the redox species above the surface of the diluent, and hence its position in the electrical double layer, can be

Received: August 7, 2012
Published: October 18, 2012

dx.doi.org/10.1021/ja307665k | J. Am. Chem. Soc. 2012, 134, 18401−18409

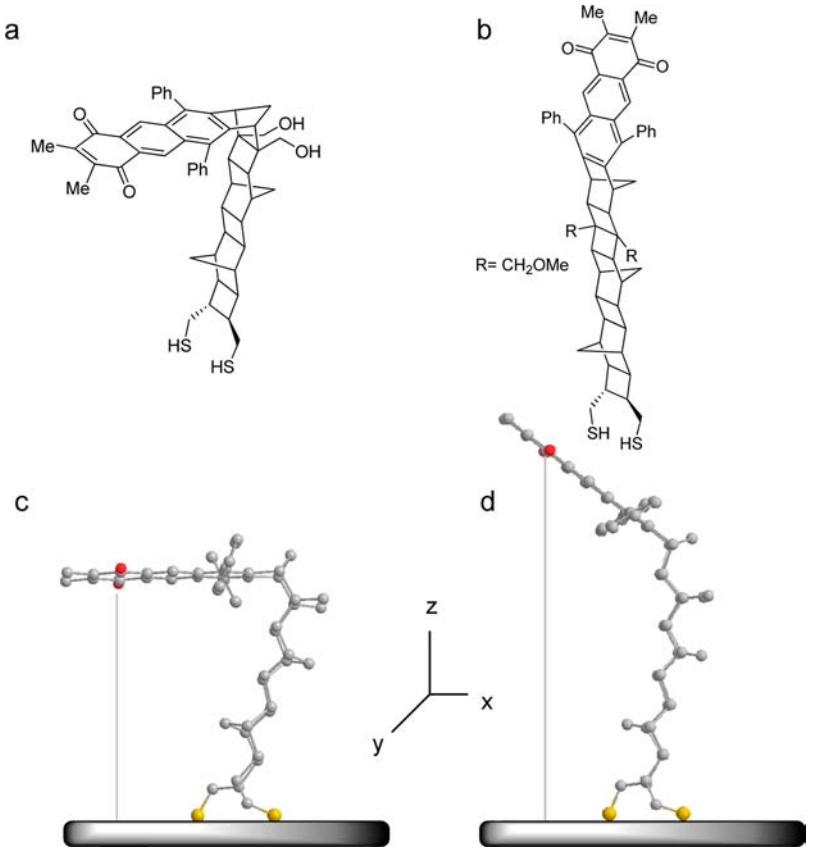

Figure 1. Chemical structure of (a) L-NB and (b) S-NB. Sketch diagrams of the orientation of the molecules on the gold surface for (c) L-NB and (d) S-NB. The molecular structures shown in this figure are B3LYP/6-31G(d) optimized geometries. The conformation of the $2CH_2SH$ groups on the surface and the tilt of the bridge both in *xz* (30°) and *yz* (25°) planes were ascertained using in situ IR spectroscopy and scanning tunneling microscopy.[19] The carbonyl groups are 13.6 and 19.8 Å away from the gold surface for the L-NB and S-NB, respectively.

precisely controlled. By changing the length of the diluent, the redox species are essentially moved through the Stern and diffuse portions of the electrical double layer.[5] In that previous study, we showed that SAMs composed of ω-hydroxyalkanethiol have a potential profile similar to that proposed for bare unmodified metal surfaces, that is, a steep drop in potential in the Stern layer followed by a smaller potential drop in the diffuse layer or the Gouy−Chapman layer, which displays an approximately exponential decay in potential out to the bulk electrolyte.[5] The electron transfer rate constant (k_{et}) was found to decrease as the distance between the ferrocene moiety and the initiation of the double layer is increased. Such a variation in k_{et} is expected for redox-active groups, which undergoes strong ion-pairing with counterions during the redox reaction, such as ferrocene.[5] However, it is possible the presence of the diluent layer can influence the electrochemistry of surface-bound species by more than just the accessibility of counterions and space charge effects as explored in our previous study. Hence, here we extend our efforts on understanding the solution environment around surface-bound redox species using new molecules where the electrochemistry does not rely so crucially on the accessibility of a strong ion-pairing counterion because both the oxidized anthraquinone and the reduced hydroanthraquinone have neutral charges.

In this Article, we turn our attention to anthraquinone moieties (AQ). AQ derivatives are exceedingly important redox-active groups due to their role in many biological systems and their potential applications in nanodevices.[6−8] AQ systems offer promise in molecular electronics as demonstrated by the electrochemical control of quantum interference.[9−11] AQ moieties undergo proton-coupled electron transfer reactions, which are critical steps in numerous natural phenomena such as photosynthesis, cellular respiration, and mitochondrial ATP synthesis.[6,12] They are typically membrane-bound, and the redox reaction occurs at the aqueous−biomembrane interface.[12] Therefore, a detailed knowledge of their redox chemistry and how the local environment affects their electron transfer properties is critical to the understanding of electron transfer in biological systems, and for designing molecular devices incorporating AQ moieties.

Unlike the ferrocene moieties, which can sense the interfacial effects at only positive potentials (potentials close to formal potential of the ferrocene/ferricinium redox couple), AQ redox reaction can be studied at a wider potential range. This is because the AQ redox reaction is pH dependent and the apparent formal potential $E^{0\prime}$can be shifted to a potential negative to the point of zero charge using solutions of high pH values as shown in eq 2.[13−15]

$$E^{0'} = E^0 - 0.0592\left[\frac{h}{n}\right]\mathrm{pH} \qquad (2)$$

where E^0 is the formal potential, and *h* and *n* are, respectively, the number of protons and electrons involved in the redox reaction. The observed $E^{0\prime}$ shifts with pH and is shifted from E^0 according to eq 2. Previous studies on AQ-terminated SAMs have shown that between pH 1 and 12.6, a 2-electron, 2-proton

dx.doi.org/10.1021/ja307665k | J. Am. Chem. Soc. 2012, 134, 18401−18409

redox reaction takes place and the $E^{0\prime}$ becomes ca. 59.2 mV more negative per increase in the pH by one unit.[16−18]

Importantly for the present work, the electron-transfer rate constant k_{et} was also found to change with pH. For example, with thiolated AQ-terminated oligo phenylene vinylene (OPV) on gold surfaces, the k_{et} was shown to increase from 9 s^{-1} at pH 1 to 647 s^{-1} at pH 12.[16] Another type of thiolated AQ-terminated OPV showed an increase in the k_{et} from 1.42 s^{-1} at pH 1 to 84.1 s^{-1} at pH 12.[19] The increase in k_{et} in basic media was attributed to a concerted electron/proton transfer, while the occurrence of a stepwise consecutive mechanism is responsible for the slower kinetics in acidic media.[16] The cyclic voltammograms of such systems were shown to exhibit an increasingly symmetrical shape of the cathodic and anodic waves as the solution became more basic.[16]

With the purpose of precisely changing the position of the AQ moiety above the surface of the monolayer, we designed a completely rigid L-shaped norbornylogous bridge (L-NB) and a straight-shaped norbornylogous bridge (S-NB) (Figure 1).[20]

The S and L-NB molecules are completely rigid and possess two CH_2SH groups at the proximal end, thereby conferring additional stability to the SAMs. On the basis of in situ IR measurements in aqueous electrolytes, the position of the anthraquinone moiety was estimated to be close to the surface tangent in the case of L-NB SAMs, and ∼45° from the surface normal in the case of S-NB SAMs.[19] Further, it was shown that both molecules do not change their orientation during the redox reaction nor when they are spaced by diluent.[20]

Using the L-NB and S-NB systems, the position of the AQ moiety can be varied across the interface that forms between the surface of the SAM and the bulk electrolyte. This can be achieved by changing the length of the diluent. Further, the environment around the AQ moieties can also be altered by changing the chemistry of the distal groups (OH or CH_3) of the diluent in mixed monolayers composed of the L-NB or the S-NB, with conventional alkanethiolate diluent.

To determine the relative orientation of the AQ moiety with respect to the surface of the diluent in mixed SAMs, sum frequency generation (SFG) vibrational spectroscopy is employed in the present study.[21−25] SFG is a second-order nonlinear optical technique that is exceedingly sensitive in probing monolayers and submonolayers on surfaces. Unlike infrared or Raman spectroscopy, SFG does not occur in homogeneous bulk media with its symmetry of inversion under electric dipole approximation and is active only at the surface or interface where symmetry of inversion is broken. Thus, SFG spectroscopy is extremely sensitive in probing the molecular structures on the surface. This technique has been widely applied in multidisciplinary research fields, including surface science, electrochemistry, materials chemistry, and biophysics, in recent years.[21−25]

In this study, we investigate the interaction of the AQ moiety in the S-NB and L-NB with the surface of the diluent in mixed monolayers using SFG technique in dried air, from which we deduced the relative position of the C═O groups of the AQ moiety relative to the surface of the diluent. We then performed electrochemical measurements in aqueous electrolytes. The length of the diluent was varied to create different positions of the AQ moiety above the surface of the SAM. The distal groups of the diluent were also varied to change the solution environment adjacent to the diluent to explore how this influenced the electron transfer behavior to the two different quinone species. The $E^{0\prime}$ and the k_{et} were measured using cyclic voltammetry (CV), alternating current voltammetry (ACV), and electrochemical impedance spectroscopy (EIS).

2. EXPERIMENTAL SECTION

Chemicals. The synthesis of the L-NB and S-NB was described previously.[20] 1-Mercapto-heptane ($6CH_3$), 1-mercapto-decane ($9CH_3$), 6-mercaptohexan-1-ol (6OH), 8-mercaptoctan-1-ol (8OH), and 9-mercaptononan-1-ol (9OH) were all purchased from Sigma Aldrich (Australia, >98%). The electrolyte used for the electrochemical measurements is sodium phosphate buffered at various pH values and adjusted to an ionic strength of 0.6 M with NaCl. For pH 4.2, the solution was prepared from H_3PO_4, NaH_2PO_4, and NaCl and adjusted with 0.1 M NaOH. For pH 6.7 and 7.8, the solution was prepared from NaH_2PO_4, Na_2HPO_4, and NaCl. For pH 9.1, the solution was prepared from NaH_2PO_4, Na_2HPO_4, and NaCl and adjusted with 0.1 M NaOH. For pH 11.4, the solution was prepared from Na_2HPO_4, Na_3PO_4, and NaCl.

Sample Preparation for SFG Experiments. The gold substrates were gold mirror electrodes prepared using a Lesker evaporator. The electrodes were prepared by evaporating a ca. 100 Å layer of titanium at a rate of 2 Å/s followed by a ca. 1000 Å layer of gold at 2 Å/s onto a 1.5 cm × 1.5 cm microscope slides. The gold slides were annealed with a hydrogen flame for about 1 min, to induce the formation of Au (111) terraces, and cooled under an atmosphere of argon, then directly transferred into the modification solution. SAMs formed from pure NB were formed by incubating the surfaces in a solution of NB (1 mM) in dichloromethane (CH_2Cl_2) for 18 h. Mixed SAMs were prepared by incubating the surfaces in a solution of NB and alkylthiolate diluent (molar ratio 1:4; total concentration 1 mM) in CH_2Cl_2. The surfaces were incubated in the mixed solution for 20 min, after which they were removed and transferred into a solution containing only the alkylthiolate (1 mM) in CH_2Cl_2 for 18 h.

Sum Frequency Generation Spectroscopy. Measurements were conducted with a broad-band femtosecond SFG system. Details of the system have been described in several reports.[26−28] Briefly, a Ti:sapphire fs laser oscillator (MaiTai, Spectra-Physics) and a regenerative amplifier (SpiteFire PRO, Spectra-Physics) pumped by a Nd:YLF laser (EMPower, Spectra-Physics) were used to generate a 2.2 mJ pulse at 800 nm with a 120 fs duration at a repetition rate of 1 kHz. One-half of the output was used to pump an optical parametric amplifier (OPA) system (TOPAS, Light Conversion) to generate IR pulses tunable from 2.5 to 10 μm with a spectral width of ca. 250 cm^{-1}. Remaining output from the amplifier was sent to a homemade spectral shaper to generate a narrow-band pulse (∼7 cm^{-1}) at 800 nm. The IR and the visible pulses were overlapped on the sample surface with incident angles of 50° and 70°, respectively. Vibrationally resolved SFG spectra were acquired with a CCD detector attached to a spectrograph. In this Article, SFG measurements were mainly focused on the C═O stretching region (1500−1800 cm^{-1}) for carbonyl group in the AQ moiety with polarization combinations of *p*-SFG, *p*-visible, and *p*-infrared (denoted as *ppp*), which is sensitive to the vibration mode perpendicular to the gold surface. The SFG measurements were performed in an environment of nitrogen to avoid any influence from water vapor in air. Further, the surfaces were incubated in dry CH_2Cl_2, which is a low dielectric constant solvent, and SFG experiments were carried out under dry nitrogen atmosphere to exclude water condensation on the monolayer from air. SFG spectra in the C−H and OH-stretching regions are presented in the Supporting Information. All SFG spectra were normalized by a SFG spectrum of a clean gold surface. A polystyrene sheet was used to calibrate the peak position of the SFG spectra.

Cyclic Voltammetry. Experiments were performed using a three-electrode cell containing a homemade gold single crystal Au (111) working electrode by forming a meniscus with the electrolyte, a platinum foil counter electrode, and an AglAgCl 3 M KCl reference electrode. The CVs were collected using a BAS 100B/W electrochemical analyzer. The single crystal Au (111) surfaces were prepared according to the method of Clavilier.[29] The detailed procedure for the fabrication of single gold crystals used in this study was reported

dx.doi.org/10.1021/ja307665k | J. Am. Chem. Soc. 2012, 134, 18401−18409

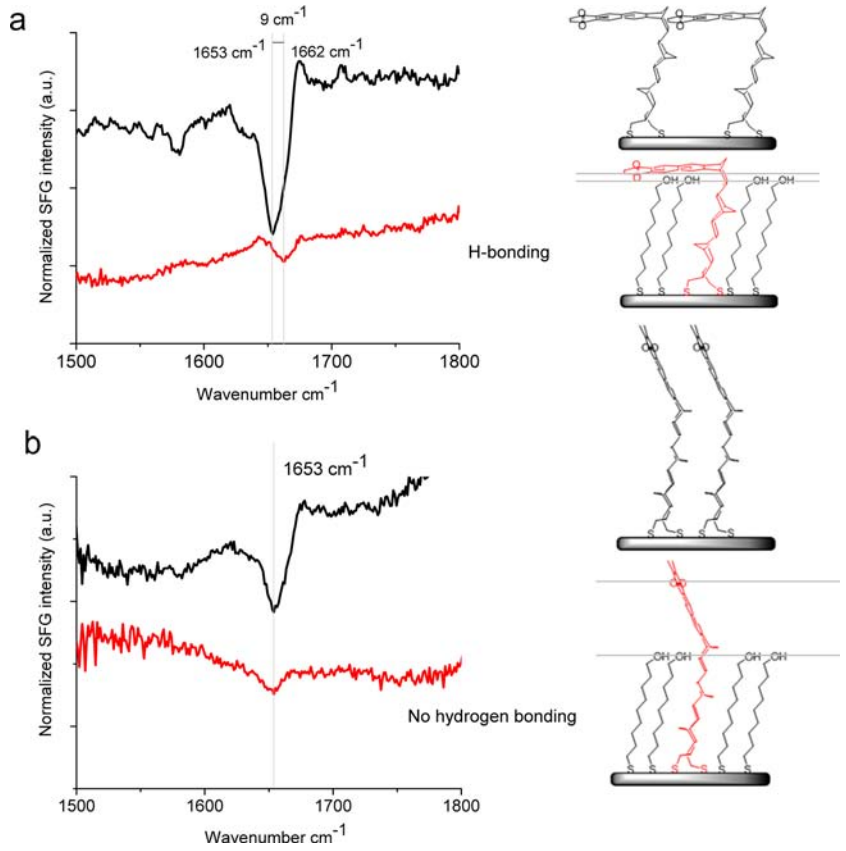

Figure 2. (a) SFG spectra in the carbonyl region of a SAM formed from L-NB as the only component and a SAM formed from L-NB mixed with 9OH diluent (L-9OH). (b) SFG spectra in the carbonyl region of a SAM formed from S-NB as the only component and a SAM formed from S-NB mixed with 9OH diluent (S-9OH). Each SFG spectrum is integrated over 60 s.

elsewhere.[30] The quality of the surfaces was assessed by CV and scanning tunneling microscopy, which were consistent with those reported for high-quality Au (111) surfaces.[30]

AC Voltammetry and Impedance Spectroscopy. The AC voltammetry and impedance spectroscopy experiments were performed using the same setup used for the CVs with a single crystal Au (111) working electrode, a platinum foil counter electrode, and an Ag| AgCl 3 M KCl reference electrode. Impedance measurements were recorded using a Solartron 1287 electrochemical interface with a Solartron Impedance/Gain-Phase Analyzer. The AC amplitude was 10 mV. Data analysis was carried out using the program Z view by Scribner Associates Inc.

Surface Modification for the Electrochemical Measurements. Mixed monolayers of the NB-alkylthiolate diluent were prepared by incubating a freshly annealed single crystal Au (111) working electrode in a solution of NB and alkylthiolate diluent (molar ratio 1:35; total concentration 1 mM) in CH_2Cl_2. The electrode was then removed from the mixed solution, rinsed thoroughly with CH_2Cl_2, and immersed in a CH_2Cl_2 solution of 1 mM alkylthiolate as the only component. This procedure was employed to separate the AQ moieties on the surface and to ensure that the dominant species on the surface are the alkylthiolate diluent. This is essential for the electrochemical measurements to eliminate lateral electron transfer that is known for SAMs containing high density of the redox-active molecules.[31,32]A low concentration of the redox-active species is also essential so that the environment around the redox-active group is dominated by the environment provided by the diluent (surface of the SAM). However, a relatively higher concentration of the redox-active molecule was essential for the SFG experiments to achieve discernible signals.

3. RESULTS AND DISCUSSION

3.1. Interaction of the AQ Moiety with Diluents in Mixed SAMs. SFG spectroscopy was employed to evaluate the interaction between the AQ moiety in the L/S NB with diluent in the mixed SAMs. The assembly of well-packed SAMs of both L-NB and S-NB have been confirmed in our previous in situ electrochemical infrared measurements in aqueous electrolyte solution.[20] The present SFG observations provide new information regarding the interaction and orientation of the L-NB/S-NB with diluent molecules in air.

First, a comparison between the position of the AQ moiety in the S-NB and L-NB was performed. For this purpose, two SAMs were constructed on the gold surface. The first is L-9OH SAM composed of L-NB and 9-mercaptononan-1-ol diluent, and the second is S-9OH SAM composed of S-NB and 9-mercaptononan-1-ol diluent. In these two SAMs, the same diluent is used; therefore, the only difference is the position of the AQ moiety with respect to the distal surface of the diluent in the mixed SAM. On the basis of the conformation of the two CH_2SH groups on the gold surface and the corresponding position of the AQ moiety that was ascertained using in situ IR spectroscopy in a previous study,[20] the L-9OH SAM will situate the C═O groups of the quinone ring at 2.1 Å away from the OH groups of the diluent (see Table S1 in the Supporting Information). However, in the S-9OH SAM, the position of the C═O groups is 8.3 Å away from the OH groups.

Figure 2 presents the *ppp*-polarized SFG spectra in the C═O region of both SAMs for (a) L-9OH and (b) S-9OH. Because of the optical interference with the nonresonant signal

dx.doi.org/10.1021/ja307665k | J. Am. Chem. Soc. 2012, 134, 18401−18409

from gold substrate, SFG peaks appear as downward on gold substrate surface, unlike those on the surface of transparent materials such as fused quartz and calcium fluoride.[26,27] The spectra are vertically shifted for clarity. The smaller SFG signal in the diluted monolayers indicates that there are less L-NB or S-NB molecules in the mixed monolayer because the intensity of the SFG signals is proportional to the square of the coverage for the target molecules. From the ratio of the SFG signals obtained from the diluted SAMs to that of the pure SAMs, the surface coverage of the diluted SAMs was estimated to be (3.25 ± 1.40) × 10^{-11} mol cm^{-2}, which represents ca. 35% of a complete surface coverage. This particular dilution condition was employed because it can physically separate the NB molecules from each other and reduce the possibility of aggregation while allowing enough NB molecules on the surface to achieve describable signals. The C═O stretching band for pure SAMs of L-NB (Figure 2a) and S-NB (Figure 2b) is observed at 1653 cm^{-1}. The SFG peak position is lower than that observed in a previous in situ IR measurement in aqueous solution (1662 cm^{-1}).[20] However, L-9OH and S-9OH clearly show different SFG peak positions. In the case of L-9OH SAM (Figure 2a), the C═O stretching band is shifted to 1662 cm^{-1}, which is blue-shifted by 9 cm^{-1}, relative to that in the pure L-NB SAM (1653 cm^{-1}). In contrast, no such shift is observed for the SAM L-9CH_3, in which the diluent hydroxy group is replaced by methyl groups (Figure 3a) as well as S-9CH_3 (Figure S4, Supporting Information). Netto-Ferreira et al. reported a similar blue-shift in the C═O frequency for the inclusion complex of 1-indanone or 2′-acetonaphone with β-cyclodextrin (ß-CD) in the solid state and interpreted in terms of highly directional H-bonding effects.[33] To explain the host−guest interaction, two opposite effects on the C═O stretching frequency due to the H-bonding result in a net blue-shift in a few wavenumbers: loss of resonance with the aromatic ring (ca. 30−40 cm^{-1} blue-shift) and decrease of the C═O force constant (ca. 15−20 cm^{-1} red-shift).[34] Similar results were also observed for an inclusion complex between Ibuprofen (IBP) and β-CD as a model system for drug delivery.[35] On the basis of these experimental and theoretical results for the hydrogen bonding in the host−guest interactions, the present findings for L-9OH SAM (Figure 2a) can be attributed to the hydrogen-bonding interactions between the proximal C═O group of the AQ moieties in L-NB with the diluent hydroxy groups. This hydrogen-bonding interaction disappears when the hydroxyl-terminated diluent is replaced by CH_3-terminated ones due to the lack of hydrogen donors (Figure 3a). Unlike the L-9OH SAM, the S-9OH SAM gave the identical C═O stretching peak position at 1653 cm^{-1} observed for the pure S-NB SAM (Figure 2b). This can be explained by the separation (8.3 Å) between the C═O groups of the AQ moieties and the diluent hydroxy groups being much larger than that for L-9OH (2.1 Å), which makes hydrogen-bonding interaction difficult to occur.

It is also interesting to note that, consistent with the above data, a blue-shift for C═O group (1662 cm^{-1}) in both L-NB and S-NB SAMs was observed in aqueous solution by our recent in situ IR measurements[20] in which hydrogen bonding of C═O group of the AQ moieties with water molecules was expected for both SAMs. A similar C═O stretching mode (1660 cm^{-1}) from AQ moieties of a quinone-terminated SAMs on gold electrodes has also been reported in aqueous solutions by in situ IR measurements.[36] Thus, in addition to the hydrogen bonding between the L-NB and hydroxyl group in the mixed OH-terminated SAMs (if the distance is suitable

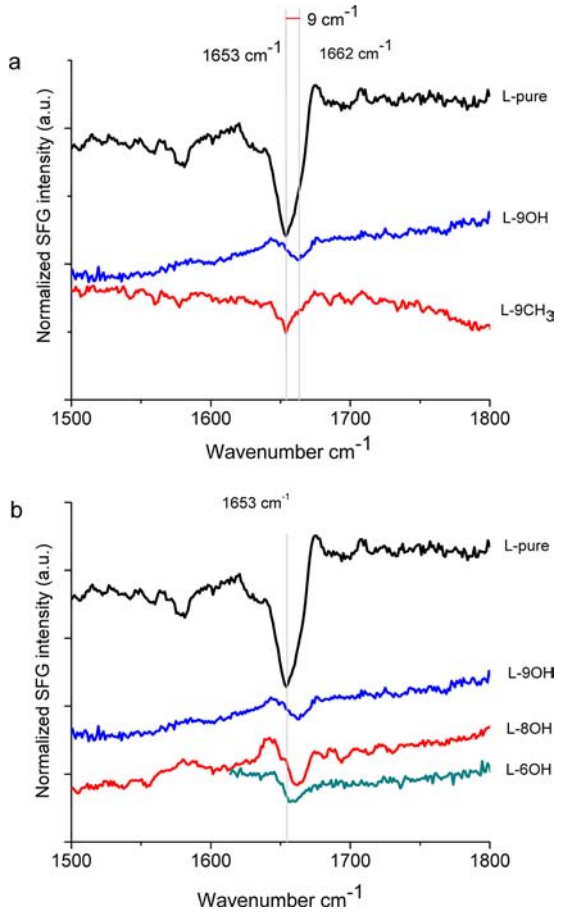

Figure 3. (a) SFG spectra in the carbonyl region of a SAM formed from L-NB as the only component (L-pure), a SAM formed from L-NB mixed with 9OH diluent (L-9OH), and a SAM formed from L-NB mixed with 9CH3 diluent (L-9CH3). (b) SFG spectra in the carbonyl region of a SAM formed from L-NB as the only component, a SAM formed from L-NB mixed with 9OH diluent (L-9OH), a SAM formed from L-NB mixed with 8OH diluent (L-8OH), and a SAM formed of L-NB mixed with 6OH diluent (L-6OH). Each SFG spectrum is integrated over 60 s.

between the C═O groups and the OH groups), AQ moieties will also interact with water molecules in aqueous electrolytes. It should be noted that unlike the S-NB, which contains CH_2OMe groups in its backbone, the L-NB contains CH_2OH groups instead (Figure 1), which can possibly be involved in H-bonding interactions with AQ in the absence of any diluent. However, the SFG results rule out this possibility because the C═O stretchings in both the pure S-NB and the pure L-NB SAMs are exactly at the same wavenumber (1653 cm^{-1}). This means that the C═O groups of the AQ moieties in the absence of OH-terminated diluent or in the absence of water (i.e., pure SAMs in dried air) are not involved in any hydrogen bonding (the stretching of a C═O involved in hydrogen bonding should be 1662 cm^{-1}). Only in the presence of OH groups in close proximity to the C═O groups, which are supplied via the diluent in air or via water (in an electrochemical cell), is the C═O wavenumber shifted to 1662 cm^{-1}.

The effect of the separation between the C═O groups, in the AQ moieties, and the diluent OH group on the magnitude of the blue-shift in the C═O frequency was examined using the series of SAMs, L-*n*OH, *n* = 6, 8, and 9. In this series, the estimated distance between the C═O groups and the OH

dx.doi.org/10.1021/ja307665k | J. Am. Chem. Soc. 2012, 134, 18401−18409

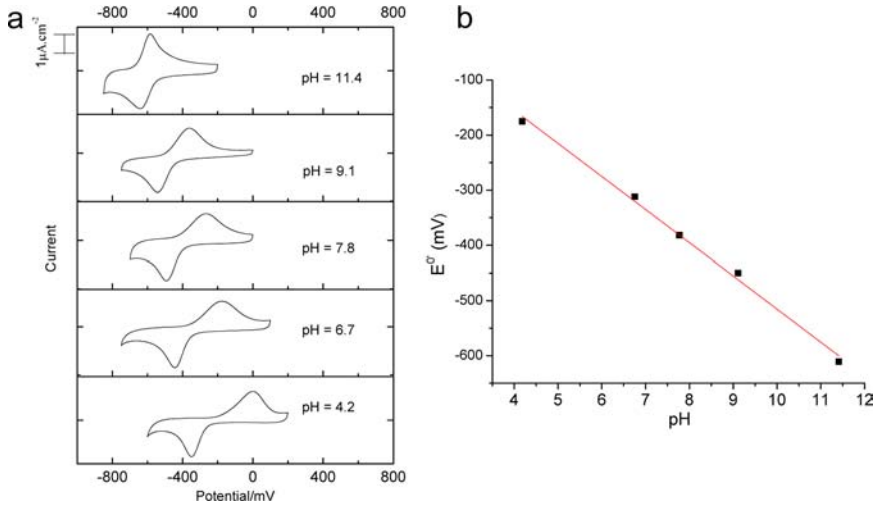

Figure 4. (a) CVs of a SAM formed from L-NB diluted with 1-mercaptononan-1-ol (L-9OH) at different pH's. (b) Evolution of the $E^{0\prime}$ with pH.

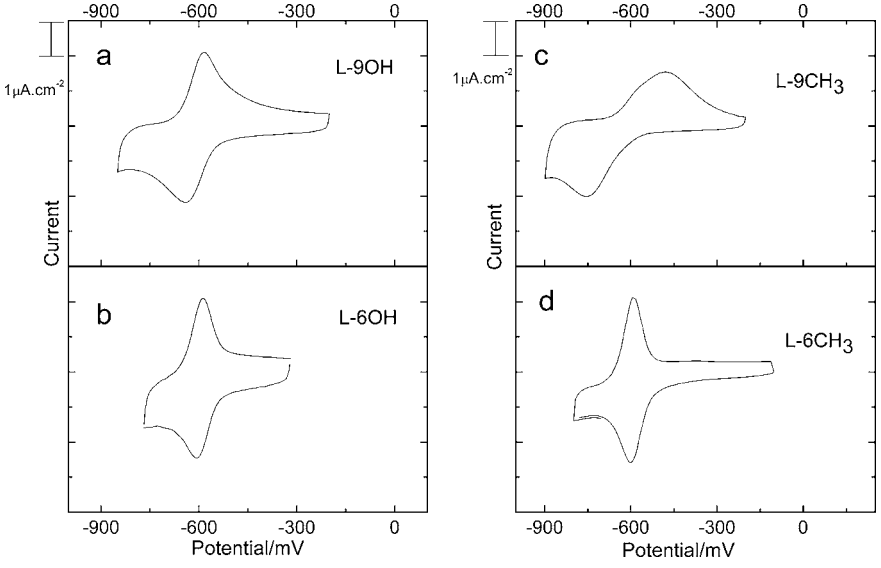

Figure 5. CVs at 50 mV/s of (a) L-9OH SAM, (b) L-6OH, (c) L-9CH_3, and (d) L-6CH_3. Measurements were performed in phosphate buffer pH = 11.4.

groups of the diluent increases with decreasing values of *n*, being 2.1, 3.2, and 5.3 Å for L-9OH, L-8OH, and L-6OH, respectively (see Table S1, Supporting Information). Figure 3b displays the SFG spectra of L-pure (1653 cm^{-1}), L-9OH (1662 cm^{-1}), L-8OH (1661 cm^{-1}), and L-6OH SAMs (1656 cm^{-1}), and it can be seen that as the length of the diluent decreases, the C═O band shifts to progressively lower frequencies. This trend is consistent with weakening of H-bonding interactions with increasing C═O···OH distance.

The above SFG results complement the estimated distances between the C═O groups and the surface of the diluent (Table S1, Supporting Information) and agrees with the orientation of the AQ moiety in the L-NB and S-NB deduced by previous in situ IR measurements in aqueous electrolytes.[20] The comparable structures of the SAMs in dry air (SFG experiments) and in aqueous electrolytes (in situ IR measurements) signify the complete structural rigidity of the SAMs whose orientation is affected neither by solvation nor by the applied potential. The SFG measurements also illustrate that the position and the environment around the AQ moieties can be changed by changing either the length of the diluent or their distal terminal groups. It particularly shows that the AQ moieties in the L-NB SAMs form a shelter, which is almost tangential to the distal groups of diluent that possess a chain length equivalent to 10 carbons (9OH or 9CH_3).

3.2. Probing the Effect of the Environment on the Redox Reaction. To probe the effect of the monolayer's environment on the AQ redox reaction, a low concentration of the AQ moiety to the diluent was employed. This is essential to ensure that the environment around the AQ moieties is mainly provided by the surface of the diluent, and the AQ moiety will act as an environmental probe only. From the area under the Faradaic waves of the CVs, the surface coverage was estimated to be $(7.1 \pm 1.2) \times 10^{-12}$ mol cm^{-2}. This translates to less than 10% of a full monolayer formed from NB as the only component ($(8.6 \pm 1.1) \times 10^{-11}$ mol cm^{-2}), which signifies that the surface modification procedure used herein ensures that the environment surrounding each AQ moiety is dominated by the diluent and prevents any lateral electron transfer between neighboring AQ moieties.

To demonstrate the dependence of the AQ redox reaction on the pH, the $E^{0\prime}$ was first measured in solutions buffered at

dx.doi.org/10.1021/ja307665k | J. Am. Chem. Soc. 2012, 134, 18401−18409

different pH values. Figure 4a shows CVs of a SAM formed from L-NB diluted with 1-mercaptononan-1-ol (L-9OH) in solutions of different pH values.

The CVs show reduction/oxidation peaks corresponding to a two-electron redox switching of the AQ redox center. The $E^{0\prime}$ shifts to more cathodic values with the increase in pH. The dependency of $E^{0\prime}$ on the pH is linear with a slope of ca. −60 mV/pH as shown in the plot in Figure 4b. (The values of $E^{0\prime}$ were obtained from the peak maximum in alternating current voltammograms (ACVs). The values obtained from ACVs match closely those obtained from the average of the anodic and cathodic waves in the CVs.)

The −60 mV/pH slope indicates that the redox reaction of the AQ moieties maintains a ($2e^-$, $2H^+$) at the entire pH range studied (4.2−11.4). The −60 mV/pH slope was found to be independent of the diluent used, and therefore a ($2e^-$, $2H^+$) redox reaction is considered for all of the systems presented in this Article. The ($2e^-$, $2H^+$) process agrees with that observed by Sato et al. for alkanethiolate SAMs.[18] The peak separation between the oxidation and the reduction waves in the CVs decreases as the pH is increased from 4.2 to 11.4. This is attributed to the increase in k_{et} with the increase in the pH values. A similar trend in the increase of the k_{et} with pH was obtained by Trammel et al. using anthraquinone-terminated oligo phenylene vinylene bridges.[16,19] A quantification of the electron transfer kinetics was obtained by calculating k_{et} using electrochemical impedance spectroscopy (EIS). The k_{et} was found to increase from 0.3 s^{-1} at pH= 4.2 to 9.5 s^{-1} at pH = 11.4. The calculation of k_{et} from EIS measurements using complex nonlinear least-squares (CNLS) fitting procedure is presented in the Supporting Information.

The effect of the solution environment on the AQ redox reaction was next investigated by changing the position of the AQ moieties relative to the distal end of the monolayer as well as by using diluent with different distal moieties at a given pH. Figure 5 presents the CVs of SAMs formed from L-NB mixed with either 9OH, 6OH, $9CH_3$, and $6CH_3$ diluent at basic pH (11.4). The k_{et} was higher for the L-6OH and L-$6CH_3$ SAMs as compared to that of the L-9OH and L-$9CH_3$ SAMs (Table 1).

Table 1. Summary of the k_{et} and $E^{0\prime}$ for the L-9OH, L-6OH, L-$9CH_3$, and L-$6CH_3$ SAMs[a]

SAM	k_{et} (s^{-1})	$E^{0\prime}$ (mV)
L-9OH (pH 11.4)	9.53 ± 0.57	−611 ± 4
L-6OH (pH 11.4)	22.25 ± 3.18	−600 ± 3
L-$9CH_3$ (pH 11.4)	3.41 ± 0.65	−622 ± 3
L-$6CH_3$ (pH 11.4)	24.85 ± 2.64	−600 ± 5
L-9OH (pH 4.2)	0.31 ± 0.05	−175 ± 5
L-6OH (pH 4.2)	0.83 ± 0.09	−165 ± 4
L-$9CH_3$ (pH 4.2)	0.11 ± 0.06	−188 ± 5
L-$6CH_3$ (pH 4.2)	0.91 ± 0.07	−163 ± 3

[a]Measurements were performed in a phosphate buffer pH 11.4 and pH 4.2.

That is, the further away the AQ moieties are from the OH or CH_3 terminated diluent, the faster is the electron transfer kinetics despite the molecule through which electrons are tunnelling (the L-NB molecule) being identical. (Evidence that the ET process occurs exclusively through the NB bridge, without modulation by the alkyl chains of neighboring diluent molecules, comes from previous ET studies[5] on mixed NB-diluent SAMs (using NB molecules of different lengths), which showed that the distance attenuation factor, β, was ca. 1.1 $bond^{-1}$ similar to the β values (0.9−1.2 $bond^{-1}$) obtained for NB bridges in solution.[5] The fact that the β-value is similar and not smaller than that observed in solution signifies that the diluent molecules are not significantly influencing the electron transfer rates in NB-diluent mixed SAMs.[5])

The $E^{0\prime}$ obtained from the peak maximum of AC voltammograms (see Figure S1, Supporting Information) was found to shift to more cathodic values in the L-9OH and L-$9CH_3$ SAMs as compared to the L-6OH and L-$6CH_3$ SAMs. A similar trend for k_{et} and $E^{0\prime}$ was also found for the same SAMs in acidic pH's (Figure 6) where k_{et} increases and $E^{0\prime}$ shifts positively for the L-6OH and L-$6CH_3$ as compared to that for the L-9OH and L-$9CH_3$ SAMs (Table 1).

The results presented in Table 1 suggest that both the thermodynamics and the kinetics of the AQ redox reaction are favored when the position of the AQ is situated away from the surface of the diluent in both basic and acidic electrolytes. First, the environmental effects on the thermodynamic quantity, $E^{0\prime}$, are considered. When the position of the AQ moiety is changed from being close to the surface (L-9OH and L-$9CH_3$) to being away from the surface (L-6OH and L-$6CH_3$), two effects related to the environmental effects on the $E^{0\prime}$ should be considered. The first is charge effects, which can contribute positively or negatively to $E^{0\prime}$ depending on the applied potential relative to the point of zero charge (*pzc*) of the diluent. The second effect is the hydrogen-bonding capability of the AQ moiety with the surrounding water, which is more accessible to the AQ when the AQ position is away from the surface as compared to the position of the AQ when it is close to the surface of the diluent. Charge effects of the diluent on the values of $E^{0\prime}$ are less likely to be the leading cause of the change in $E^{0\prime}$. This is because in both acidic and basic pH's a positive shift in $E^{0\prime}$ is observed when the AQ moieties are situated away from the surface. If the shifts for $E^{0\prime}$ are due to charge effects, then the magnitude of this shift would be expected to diminish or to be inversed when applying a potential close to the *pzc* of the diluent. However, as seen in acidic pH's, the positive shifts in $E^{0\prime}$ are still observed for the L-6OH and L-$6CH_3$ SAMs at which the apparent formal potential is close to the suggested *pzc* of the diluent (e.g., *pzc* for hydroxyl terminated diluent is ca. −110 mV vs Ag/AgCl).[37] This suggests that the leading cause of the positive shift in $E^{0\prime}$ for the L-6OH and L-$6CH_3$ SAMs is the greater hydrogen-bonding interactions of the AQ moieties with water in these two SAMs. Recent X-ray and neutron reflectometry studies have shown that, adjacent to the distal surface of a monolayer, there exist a low-water density layer of few angstroms thick as compared to that in the bulk solution.[38−40] The water density of this layer decreases further with an increase in the hydrophobicity of the monolayer. Therefore, it is likely that the AQ moieties in the L-9OH and L-$9CH_3$ SAMs have less access to water as compared to the L-6OH and L-$6CH_3$ SAMs, and therefore a stronger hydrogen-bonding interaction is expected for the latter SAMs, which facilitates the reduction of the AQ causing a positive shift in the $E^{0\prime}$. Positive shift in the $E^{0\prime}$ was recently demonstrated for quinone species in solution by a study performed by Webster and co-workers,[41] which showed that the two reduction peaks of the quinone in dry organic solvents, representing the mono and dianions, shift to more positive potentials upon the addition of water.

More recently, it was demonstrated by Hankache et al.[42] that hydrogen bonding of anthraquinone with water also enhances

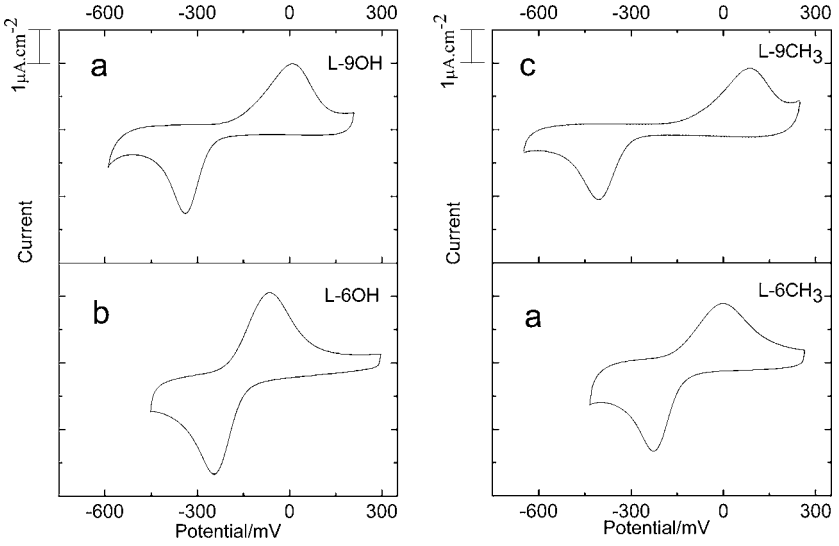

Figure 6. CVs at 50 mV/s of (a) L-9OH SAM, (b) L-6OH, (c) L-9CH_3, and (d) L-6CH_3. Measurements were performed in phosphate buffer pH = 4.2.

the kinetics of electron transfer. In the paper of Hankache et al., it was demonstrated that the rate of photoinduced electron transfer in a ruthenium−bridge−anthraquinone dyad increases markedly upon addition of hydrogen-bond donors that can bind to the anthraquinone unit.[42] Particularly, the rates of intramolecular electron transfer are higher in acetonitrile/water mixture than in dry acetonitrile. Further, water interaction effects were also suggested for explaining the increase in the molecular conductance of conjugated thiophene-based gold−molecule−gold junctions by several folds as compared to the conductance of the same molecule in anhydrous organic solvents.[43] In this vein, the increase in the k_{et} in the L-6OH and L-6CH_3 SAMs can be attributed to an enhanced interaction with water in these two SAMs as compared to a weaker interaction with water due to the position of the AQ with the surface of the diluent in the L-9OH and L-9CH_3 SAMs. It is also noted that the L-9CH_3 SAM showed the lowest k_{et} values, which can be explained by the position of the AQ moiety in this SAM (CH_3 terminated) being situated in the most hydrophobic environment and thus have the least interaction with water molecules among the four SAMs.

Another approach that was employed to change the position of the AQ moieties relative to the distal surface of the SAM is comparing the S-NB and L-NB systems using the same diluent (Figure 7). It was shown in the SFG section that the L-NB molecule situates the AQ moiety almost tangential to the surface of the diluent, while in the S-NB the AQ moiety is almost 45° from the surface normal. Therefore, in the S-9CH_3 SAM, the quinone ring is being lifted away from the surface of the monolayer.

As expected, the k_{et} was found to be higher, and the $E^{0\prime}$ shifts to more positive potentials for the S-9CH_3 SAM in which the position of the AQ moieties allows the quinone moiety (the ring that undergoes most of the change during the electrochemical reaction) to enjoy access to water molecules as compared to the L-9CH_3 SAM in which the parallel orientation of the AQ essentially situates the quinone ring in an area of lower water density (Table 2). Further, the effect of 9OH and 9CH_3 diluents on the S-NB was investigated. Although these two diluents have different distal groups, they did not affect considerably the $E^{0\prime}$ and the k_{et} of the S-NB molecule. This is

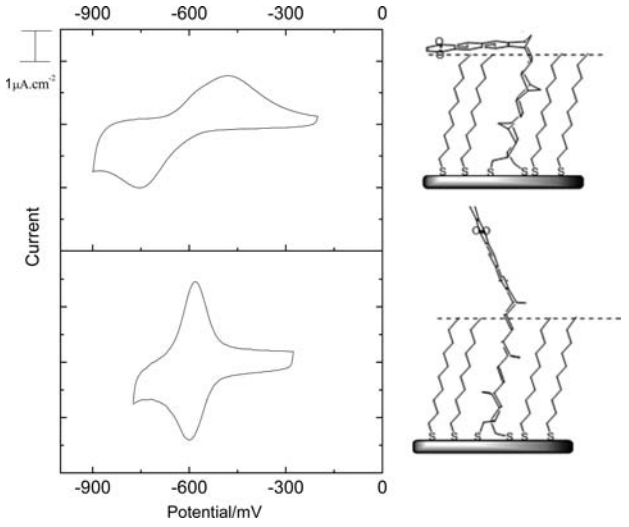

Figure 7. CVs at 50 mV/s of (a) L-9CH_3 SAM and (b) S-9CH_3. Measurements were performed in phosphate buffer pH = 11.4.

Table 2. Summary of the k_{et} and $E^{0\prime}$ for the S-9CH_3, L-9CH_3, and L-9OH SAMs[a]

SAM	k_{et} (s^{-1})	$E^{0\prime}$ (mV)
S-9CH_3	33.48 ± 4.65	−600 ± 5
L-9CH_3	3.41 ± 0.65	−622 ± 3
S-9OH	35.14 ± 7.35	−595 ± 6

[a]Measurements were performed in a phosphate buffer pH = 11.4.

attributed to the considerable distance (8.3 Å) between the carbonyl groups of the AQ moiety and the distal surface of the diluent. These results show that the influence of the diluent on the redox reaction is considerable only when the diluents are in close proximity to the AQ moieties and the redox reaction is not affected when the AQ moieties are situated in a uniform and similar environment that is dominated by the bulk solution.

4. CONCLUSION

We demonstrated using rigid norbornylogous bridges that the position of the AQ moiety relative to the surface of a self-

assembled monolayer has a significant influence on the AQ redox reaction. We first deduced the position of the AQ moieties from their interaction with the distal groups of the diluent using SFG vibrational spectroscopy in air. It was shown that the AQ moiety forms a shelter over the surface of the diluent in the L-NB, while the AQ moieties are oriented relatively closer to the surface normal in case of the S-NB. In aqueous electrolytes, the $E^{0\prime}$ was found to shift positive when the AQ moiety is situated away from the distal surface of the diluent, and this occurs for diluent terminated with hydrophilic (OH) groups or hydrophobic (CH_3) groups. The k_{et} was found to increase when the AQ moiety is situated away from the surface of the diluent, and this occurs more prominently in the case of the CH_3-terminated diluent, which is attributed to the more hydrophobic environment that the CH_3-terminated diluent provides. We propose that the presence of a low-water density layer adjacent to a monolayer surface can be sensed using the AQ redox reaction. Thus, this study contributes to the discussion of the existence of this low-water density layer. This time we show the influence of this low-water density layer on redox reactions involved as part of a self-assembled monolayer.

■ ASSOCIATED CONTENT

Ⓢ Supporting Information

Distances between the C═O of the AQ moiety and the surface of the diluent; AC voltammograms; rate constant calculation using EIS; SFG spectra of S-pure versus S-9CH3; and SFG spectra in the C−H and O−H stretching region. This material is available free of charge via the Internet at http://pubs.acs.org.

■ AUTHOR INFORMATION

Corresponding Author

justin.gooding@unsw.edu.au; m.paddonrow@unsw.edu.au; ye@cat.hokudai.ac.jp

Notes

The authors declare no competing financial interest.

■ ACKNOWLEDGMENTS

N.D. acknowledges ARCNN for a travel fellowship to Hokkaido University, Japan. The Australian Research Council under the Discovery Projects Funding Scheme is acknowledged. This work was partially supported by Grant-in-Aid for Scientific Research (B) 23350058 and Grant-in-Aid for Scientific Research on Innovative Areas "Coordination program" 24108701 from MEXT, Japan.

■ REFERENCES

(1) Eckermann, A. L.; Feld, D. J.; Shaw, J. A.; Meade, T. J. *Coord. Chem. Rev.* **2010**, *254*, 1769−1802.
(2) Gooding, J. J.; Darwish, N. *Chem. Rec.* **2012**, *12*, 92−105.
(3) Smith, C. P.; White, H. S. *Anal. Chem.* **1992**, *64*, 2398−2405.
(4) Fawcett, W. R. *Electroanal. Chem.* **1994**, *378*, 117.
(5) Eggers, P. K.; Darwish, N.; Paddon-Row, M. N.; Gooding, J. J. *J. Am. Chem. Soc.* **2012**, *134*, 7539−7544.
(6) Trumpower, B. L. *J. Biol. Chem.* **1990**, *265*, 11409−11412.
(7) Gómez, M.; González, F. J.; González, I. *Electroanal. Chem.* **2005**, *578*, 193−202.
(8) van Dijk, E. H.; Myles, D. J. T.; van der Veen, M. H.; Hummelen, J. C. *Org. Lett.* **2006**, *8*, 2333−2336.
(9) Darwish, N.; Díez-Pérez, I.; Da Silva, P.; Tao, N.; Gooding, J. J.; Paddon-Row, M. N. *Angew. Chem., Int. Ed.* **2012**, *51*, 3203−3206.
(10) Fracasso, D.; Valkenier, H.; Hummelen, J. C.; Solomon, G. C.; Chiechi, R. C. *J. Am. Chem. Soc.* **2011**, *133*, 9556−9563.
(11) Darwish, N.; Díez-Pérez, I.; Guo, S.; Tao, N.; Gooding, J. J.; Paddon-Row, M. N. *J. Phys. Chem. C* **2012**, *116*, 21093−21097.
(12) Matsson, M.; Tolstoy, D.; Aasa, R.; Hederstedt, L. *Biochemistry* **2000**, *39*, 8617−8624.
(13) Quan, M.; Sanchez, D.; Wasylkiw, M. F.; Smith, D. K. *J. Am. Chem. Soc.* **2007**, *129*, 12847−12856.
(14) Laviron, E. *Electroanal. Chem.* **1984**, *169*, 29−46.
(15) Finklea, H. O. *J. Phys. Chem. B* **2001**, *105*, 8685−8693.
(16) Trammell, S. A.; Lowy, D. A.; Seferos, D. S.; Moore, M.; Bazan, G. C.; Lebedev, N. *Electroanal. Chem.* **2007**, *606*, 33−38.
(17) Hong, H.-G.; Park, W. *Langmuir* **2001**, *17*, 2485−2492.
(18) Sato, Y.; Fujita, M.; Mizutani, F.; Uosaki, K. *Electroanal. Chem.* **1996**, *409*, 145−154.
(19) Trammell, S. A.; Moore, M.; Schull, T. L.; Lebedev, N. *Electroanal. Chem.* **2009**, *628*, 125−133.
(20) Darwish, N.; Eggers, P. K.; Da Silva, P.; Zhang, Y.; Tong, Y.; Ye, S.; Gooding, J. J.; Paddon-Row, M. N. *Chem.-Eur. J.* **2012**, *18*, 283−292.
(21) Shen, Y. R. *Nature* **1989**, *337*, 519−525.
(22) Shen, Y. R.; Ostroverkhov, V. *Chem. Rev.* **2006**, *106*, 1140−1154.
(23) Richmond, G. L. *Chem. Rev.* **2002**, *102*, 2693−2724.
(24) Holman, J.; Davies, P. B.; Nishida, T.; Ye, S.; Neivandt, D. J. *J. Phys. Chem. B* **2005**, *109*, 18723−18732.
(25) Ye, S.; Osawa, M. *Chem. Lett.* **2009**, *38*, 386−391.
(26) Ye, S.; Noda, H.; Morita, S.; Uosaki, K.; Osawa, M. *Langmuir* **2003**, *19*, 2238−2242.
(27) Ye, S.; Noda, H.; Nishida, T.; Morita, S.; Osawa, M. *Langmuir* **2004**, *20*, 357−365.
(28) Tong, Y.; Li, N.; Liu, H.; Ge, A.; Osawa, M.; Ye, S. *Angew. Chem., Int. Ed.* **2010**, *49*, 2319−2323.
(29) Clavilier, J.; Faure, R.; Guinet, G.; Durand, R. *J. Electroanal. Chem. Interfacial Electrochem.* **1979**, *107*, 205−209.
(30) Darwish, N. A.; Eggers, P. K.; Yang, W.; Paddon-Row, M. N.; Gooding, J. J. *Nanoscience and Nanotechnology (ICONN), 2010 International Conference*, Feb. 22−26, 2010; pp 302−305.
(31) Chidsey, C. E. D.; Bertozzi, C. R.; Putvinski, T. M.; Mujsce, A. M. *J. Am. Chem. Soc.* **1990**, *112*, 4301−4306.
(32) Dodzi, Z.; Cyril, H.; Luc, S.; Marcel, G.; Bruno, F.; Philippe, H.; Han, Z. *Angew. Chem., Int. Ed.* **2010**, *49*, 3157−3160.
(33) Netto-Ferreira, J. C.; Ilharco, L. M.; Garcia, A. R.; Vieira Ferreira, L. F. *Langmuir* **2000**, *16*, 10392−10397.
(34) Li, G.; Ye, S.; Morita, S.; Nishida, T.; Osawa, M. *J. Am. Chem. Soc.* **2004**, *126*, 12198−12199.
(35) Crupi, V.; Majolino, D.; Venuti, V.; Guella, G.; Mancini, I.; Rossi, B.; Verrocchio, P.; Viliani, G.; Stancanelli, R. *J. Phys. Chem. A* **2010**, *114*, 6811−6817.
(36) Ye, S.; Yashiro, A.; Sato, Y.; Uosaki, K. *J. Chem. Soc., Faraday Trans.* **1996**, *92*, 3813−3821.
(37) Becka, A. M.; Miller, C. J. *J. Phys. Chem.* **1993**, *97*, 6233−6239.
(38) Poynor, A.; Hong, L.; Robinson, I.; Granick, S.; Zhang, Z.; Fenter, P. *Phys. Rev. Lett.* **2006**, *97*, 22601−22604.
(39) Mezger, M.; Sedlmeier, F.; Horinek, D.; Reichert, H.; Pontoni, D.; Dosch, H. *J. Am. Chem. Soc.* **2010**, *132*, 6735−6741.
(40) Maccarini, M.; Steitz, R.; Himmelhaus, M.; Fick, J.; Tatur, S.; Wolff, M.; Grunze, M.; Janeček, J.; Netz, R. R. *Langmuir* **2006**, *23*, 598−608.
(41) Hui, Y.; Chng, E. L. K.; Chng, C. Y. L.; Poh, H. L.; Webster, R. D. *J. Am. Chem. Soc.* **2009**, *131*, 1523−1534.
(42) Hankache, J.; Hanss, D.; Wenger, O. S. *J. Phys. Chem. A* **2012**, *116*, 3347−3358.
(43) Leary, E.; et al. *Phys. Rev. Lett.* **2009**, *102*, 086801.